Modeling Dead Space in Measurements of Pulmonary Ventilation Using Hyperpolarized 3He MRI

K. Emami[1], M. Ishii[1,2], S. Kadlecek[1], J. MacDuffie-Woodburn[1], J. Zhu[3], S. Pickup[1], J. Yu[1], M. Stetz[1], M. Stephen[4], and R. Rizi[1]

[1]Radiology, University of Pennsylvania, Philadelphia, PA, United States, [2]Department of Otolaryngology â€“ Head and Neck Surgery, Johns Hopkins University, Baltimore, MD, United States, [3]Division of Thoracic Surgery, University of Pennsylvania, Philadelphia, PA, United States, [4]Pulmonary, Allergy, and Critical Care Division, University of Pennsylvania, Philadelphia, PA, United States

INTRODUCTION: The dead space volume in measurements of lung ventilation using gaseous contrast agents (e.g. hyperpolarized ^{3}He) can be a substantial source of error if their magnitude is not carefully incorporated in the gas distribution model. The dead space in lung ventilation can be divided into two main components (Figure 1.a): (1) *Dynamic Dead Volume*, V_D: contains the major conductive airways and the portion of the ventilator after the respirator valve, including endotracheal tube which experiences a bi-directional flow during respiration; (2) *Static Dead Volume*, V_S: contains part of the ventilator system that only uni-directionally carries the source contrast gas towards the respirator valve's inlet, primarily containing the transmission line between the ^{3}He chamber and the respirator valve. The primary distinction between V_D and V_S is that the portion of the respiratory gas residing in V_D from the previous breath is re-inhaled with each new breath; known as *rebreathing*.

METHODS: <u>THEORY:</u> A lumped three-compartment model is proposed as illustrated in Figure 1.b to model the system dead volumes. The rightmost compartment comprises the acinar airways and contains the magnetization M_A; the middle compartment comprises the combination of major conductive airways and the respiratory valve, and contains the magnetization M_C; and the leftmost compartment includes the transmission line (with magnetization M_T) that carries the HP ^{3}He from the source (M_S). For the serial ventilation sequence [1], the magnetization buildup can be expressed as: $M_A(j) = r \cdot M_T(j-1) + (1-r) \cdot M_A(j-1) \cdot \exp\left[D_{RF} + D_{O_2}\right]$ where $r = r_A \cdot (1-r_D)$ is the *apparent fractional ventilation*, including the rebreathing effect of conductive airways, and $r_D = V_D/V_T$. The RF and oxygen decay mechanisms are governed by $D_{RF} = N_{PE} \ln(\cos\alpha)$ and $D_{O2} = -\tau/T_{1,O2}$, with $T_{1,O2}$, $= \xi/PO_2$. It is implied that the arriving magnetization from the conductive airways, M_C, at each breath is a combination of the arriving HP ^{3}He from the transmission line and the exhaled gas from the previous breath. Since the gas in the transportation line travels only in one direction towards the respiratory valve, it is assumed that the entrance of HP ^{3}He gas from the source pushes the same amount of gas (V_T) out of the static dead volume (Figure 1.c). For a relatively small V_T compared to V_S ($r_S = V_T/V_S < 1$, e.g. in rodents), the concentration of the gas delivered from the transmission line M_T, incrementally increases with each breath. However for large tidal volumes ($r_S > 1$, e.g. in humans), the entire contents of the static dead space is purged with the first breath. <u>SIMULATION:</u> The magnetization and signal build-up history in acinar airways were simulated using: M_S = 1 [a.u.], N = 30, τ = 1 s, N_{PE} = 64, P_S = 140 mbar, V_T = 2 ml, and V_R = 6 ml. All initial magnetizations are zero. Introduction of the two types of dead space affects the magnetization and signal build-up in very different ways (not shown). Adding V_D to a no-dead-space system (r_D=0 and r_S=∞) is reflected as a lower steady state magnetization, M_∞, and a lower apparent fractional ventilation. Introduction of V_S to a no-dead-space system, on the other hand, increases the rise time of magnetization build-up curve. This curve however eventually reaches the same M_∞ as that of the no-dead-space system. <u>PHANTOM:</u> An artificial lung phantom was constructed with a 10-ml glass syringe (ID=1.46cm), loaded with a nonmagnetic beryllium-copper compression spring (3.24" free length @ 0.145 lb/in). A residual volume of V_R = 4 ml was enforced. The syringe-spring assembly was ventilated with three different tidal volumes V_T = 1.1, 2.5 and 4.5 ml (equivalent to $r_A = V_T/(V_T+V_R)$ = 0.22, 0.38 and 0.53). Dead spaces were directly measured as $V_D \approx$ 0.5 ml and $V_S \approx$ 3.2 ml. Imaging was performed using a GEMS pulse sequence on a 50-cm 4.7-T MRI scanner equipped with 12-cm 25 G/cm gradients and a quadrature 8-leg birdcage body coil (152.95 MHz, ID=7cm), with: projections at FOV=6×6cm^2, α = 4~5°, MS=64×64 pixels, T_R=6.6 ms and T_E=3.3 ms.

RESULTS: Fractional ventilation was measured in the spring-syringe setup with each measurement repeated three times. The experimental results (0.22, 0.37 and 0.52) were in good agreement with *a priori* r_A values. The fractional ventilation r_A and dynamic dead space ratio r_D are related through $r = r_A \cdot (1-r_D)$. Therefore the relative error in r_A as a function of uncertainty in r_D is governed by $\Delta r_A = \delta r_A / r_A = \delta r_D$. The constructed model with a nominal r_S = 0.3 and above parameters, were solved numerically for the unknown r_A and $r_S \in$ [0.0, 0.9] and the relative error Δr_A was calculated (Figure 2.a), showing a monotinc dependence of Δr_A on r_S variation. The relative error is larger for smaller r_A values. For instance, an error of +0.05 in r_S results in 80% overestimation of r_A = 0.15, whereas it only affects r_A = 0.45 by 45%. The sensitivity of the model was also assessed to entirely ignoring static dead space using $r_S \in$ [0.1, 10] and solving for r_A by setting $r_S \to \infty$. The net result of ignoring V_S is underestimation of r_A value, again with a larger relative error for smaller r_A values. The model however quickly becomes less sensitive as the actual r_S value grows beyond ~ 6 (Figure 2.b).

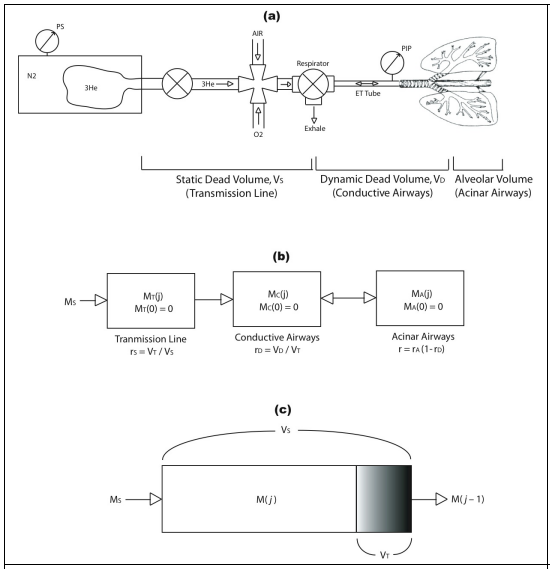

Figure 1. (a) Schematic diagram of the mechanical ventilator depicting the static and dynamic dead space volumes; **(b)** three-compartment lumped model of dead space volumes; and **(c)** details of gas replacement model in the static dead space compartment.

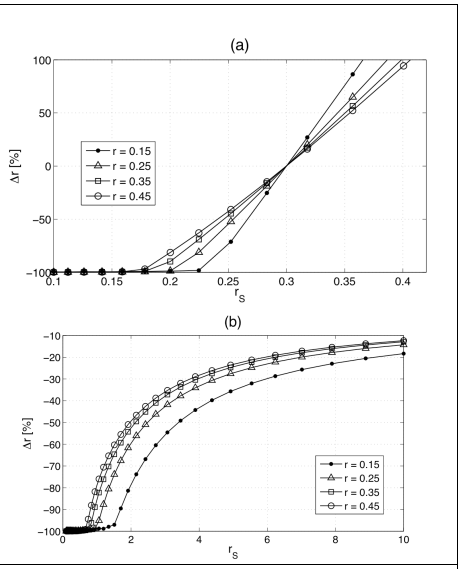

Figure 2. Sensitivity of the ventilation measurements (r_A) to **(a)** incorrect assumption of static dead space value; **(b)** ignoring static dead space.

DISCUSSION: Simulation and experimental results both indicate that inclusion of dead space volume in the ventilation model allows for a better fit to the data by providing additional degrees of freedom to the signal buildup model. As shown in simulation, as well as the syringe phantom experiment, in presence of a static dead volume, the signal buildup curve starts resembling an *S*-shaped curve. In the absence of the static dead space model the signal buildup curve is mathematically incapable of exhibiting such a behavior and therefore adversely affects the estimation of r_A value. This model has a greater significance in small animals and rodents where the tidal volume is of the same order of magnitude as dynamic and static dead space volumes. On the other hand it, is important to note that inaccurate estimation of system dead volumes can lead to error in r_A calculation as well, and therefore it is necessary to balance the tradeoff between the two factors through direct and accurate measurement of system dead spaces and estimating the volume of major conductive airways in the imaged subject.

REFERENCES: [1] Emami K, *et al.* A Novel Approach to Measure Regional Lung Ventilation Using Hyperpolarized 3He MRI – Potential in Clinical Studies; ISMRM 16th Scientific Meeting, Berlin, Germany: May 2007.